Multiple method analysis of TiO_2 nanoparticle uptake in rice (*Oryza sativa* L.) plants

Yingqing Deng[a,†], Elijah J. Petersen[b,†,*], Katie Challis[c], Savelas A. Rabb[d], R. David Holbrook[e], James F. Ranville[c], Bryant C. Nelson [b], Baoshan Xing[a,*]

[a] Stockbridge School of Agriculture, University of Massachusetts Amherst, Amherst, Massachusetts 01003, United States

[b] Biosystems and Biomaterials Division, National Institute of Standards and Technology, Gaithersburg, Maryland 20899, United States

[c] Department of Chemistry and Geochemistry, Colorado School of Mines, Golden, Colorado 80401, United States

[d] Chemical Sciences Division, National Institute of Standards and Technology, Gaithersburg, Maryland 20899, United States

[e] Materials Measurement Science Division, National Institute of Standards and Technology, Gaithersburg, Maryland 20899, United States

[†] **Both authors contributed equally to this work.**

***Corresponding authors:**

E.J.P., e-mail address: elijah.petersen@nist.gov; Tel: 301-975-8142; Address: National Institute of Standards and Technology, 100 Bureau Dr., Building 227 Room A222, Gaithersburg, MD, USA 20899

B.S.X, e-mail address: bx@umass.edu, Tel: 413-545-5212, Address: University of Massachusetts, Stockbridge School of Agriculture, 410 Paige Lab, Amherst, MA, USA 01003

Abstract

Understanding the translocation of nanoparticles (NPs) into plants is challenging because qualitative and quantitative methods are still being developed and the comparability of results among different methods is unclear. In this study, uptake of titanium dioxide NPs and larger bulk particles (BPs) at 5 mg/L and 50 mg/L concentrations in rice plant (*Oryza sativa L.*) tissues was evaluated using three orthogonal techniques: electron microscopy, single-particle inductively coupled plasma mass spectroscopy (spICP-MS) with two different plant digestion approaches, and total elemental analysis using ICP optical emission spectroscopy. In agreement with electron microscopy results, total elemental analysis of plants exposed to TiO_2 NPs and BPs at 5 mg/L and 50 mg/L concentrations revealed that TiO_2 NPs penetrated into the plant root and resulted in Ti accumulation in above ground tissues at a higher level compared to BPs. spICP-MS analyses revealed that the size distributions of internalized particles differed between the NPs and BPs with the NPs showing a distribution with smaller particles. Acid digestion resulted in higher particle numbers and the detection of a broader range of particle sizes than the enzymatic digestion approach, highlighting the need for development of robust plant digestion procedures for NP analysis. Overall, there was agreement among the three techniques regarding NP and BP penetration into rice plant roots and spICP-MS showed its unique contribution to provide size distribution information.

Key words: titanium dioxide nanoparticles, plant uptake, bioaccumulation, rice, single particle ICP-MS, electron microscopy

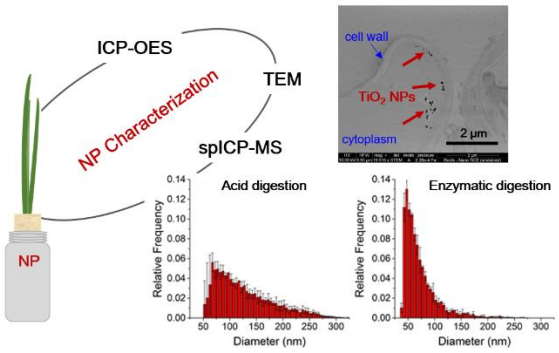

TOC artwork

Introduction

Nanotechnology is expected to impact a wide range of industries, and the incorporation of nanomaterials into commercial products is expected to continue increasing in future years. For example, TiO_2 nanoparticles (NPs), are extensively incorporated into a large variety of commercial products, including sunscreens/cosmetics, gas sensors, pigments/coatings, construction materials (e.g. cements), food additives, drugs, and agrochemical sprays.[1, 2] As a result of release from nano-enabled products, the concentration of TiO_2 NPs has been predicted to reach 16 µg/L in surface water and 0.47 mg/kg in sludge-treated soil, concentrations much higher than those predicted for ZnO NPs, Ag NPs, carbon nanotubes or fullerenes.[3-6] In the environment, potential accumulation of TiO_2 NPs into plants may introduce these NPs into the food chain. In addition, TiO_2 NPs and SiNPs have been investigated to support the development of plants by reducing abiotic stress and decreasing uptake of co-contaminants.[7-9] Therefore, in order to identify and evaluate possible risks in food safety, fundamental information is needed regarding the interactions between TiO_2 NPs and plants and robust analytical methods are needed to quantify uptake and translocation of TiO_2 NPs into plants.

Though a growing number of studies are emerging on NPs interacting with terrestrial plants, available analytical techniques and associated sample pretreatment methods are limited for assessing the NPs within biological tissues. Some of the most frequently used detection techniques for NPs in plant tissues are electron microscopy (EM), X-ray absorption spectroscopy (XAS), surface enhanced Raman scattering (SERS), and total elemental analysis methods.[10-13] An early study used 2.8 nm Alizarin red S-bound (ARS) TiO_2 NPs to test the uptake potential in *Arabidopsis* seedlings.[14] However, the surface sites of these TiO_2 NPs were saturated with sucrose before ARS-labeling, which may have modified the NP uptake potential. Compared to dye labelling, EM coupled with an energy dispersive X-ray spectroscopy (EDS) detector can provide direct visualization of nanomaterials and qualitative determination of their elemental compositions.[15-17] In a more recent study involving TiO_2 NPs with diameters from 14 nm to 655 nm, a threshold

diameter of 140 nm was reported as the upper size limit for wheat uptake using a combination of techniques including scanning electron microscopy (SEM) and XAS.[15] Although this study reported that TiO_2 NPs did not undergo *in vivo* crystal phase modification, the mechanistic explanation describing how the TiO_2 NPs were taken up into the plants was not fully explained.[15] In addition to transmission electron microscopy (TEM)-EDS, synchrotron X-ray florescence microscopy is becoming more frequently used for *in situ* mapping and determination of the speciation of NPs in plant tissues.[18] However, results from both TEM and XAS analyses are usually qualitative or semi-quantitative because of the substantial amount of tissue that would need to be analyzed for quantitative NP concentration results. While total elemental analysis does provide quantitative information about the total concentration of specific elements in plant tissue, this technique only detects Ti and therefore cannot distinguish between background Ti in the plant and uptake of TiO_2 NPs. Overall, the methods used to date do not provide quantitative information about uptake of TiO_2 NPs by plants, and the comparability of different measurement techniques for assessing the uptake of TiO_2 NPs into plants is unclear.

One promising analytical technique for quantifying the size distribution of NPs in biological samples is single particle inductively coupled plasma-mass spectrometry (spICP-MS). This technique has been recently used to analyze the size distribution of gold NPs and cerium dioxide NPs in plants.[19, 20] However, to our knowledge, spICP-MS has not yet been used for assessing TiO_2 NPs in any organism, although spICP-MS has been used to quantify titania NPs in other environmentally relevant matrices.[21-23] The spICP-MS technique utilizes time-resolved isotopic analysis with short dwell times to characterize the particle size distribution and particle number concentration in samples.[24-27] However, the application of spICP-MS in environmentally/biologically-relevant samples is still largely limited by uncertainty in the robustness of different extraction methods and interferences from natural matrices.

In the present study, uptake of TiO_2 NPs in hydroponically grown rice plants was comprehensively evaluated using three orthogonal techniques. After the exposure period, plants

were evaluated using EM and bulk elemental analysis of acid extracts via inductively coupled plasma-optical emission spectroscopy (ICP-OES). A newly developed spICP-MS method was also applied to the extracts obtained with two different extraction methods (enzymatic and acidic). The comparability of the results from the different methods was evaluated.

Materials and methods

Characterization of TiO_2 particles

TiO_2 NPs (SRM 1898, 99.5 % purity) were acquired from the National Institute of Standards and Technology (NIST; Gaithersburg, MD) with primary particle sizes from 19 nm to 37 nm and a mixed-phase crystal structure consisting of anatase and rutile polymorphs. The specific surface area of SRM 1898 has been previously characterized as (55.55 ± 0.70) m^2/g.[28, 29] Elementally similar TiO_2 bulk particles (BPs, purity 98.0 % to 100.5 %) were purchased from Acros Organics (New Jersey, USA). The hydrodynamic size and zeta potential of TiO_2 NPs were measured in deionized water using dynamic light scattering (DLS, Zetasizer Nano, Malvern) shortly prior to exposure. The intensity-based hydrodynamic diameters were measured using 173° backscatter detection at 25 ºC; at least three replicates were tested per condition and each run had at least 3 sub-runs. For all plant experiments, the TiO_2 NP and BP suspensions were prepared in Milli-Q water at 5 mg/L and 50 mg/L and dispersed with a probe sonicator (Misonix S-4000, Farmingdale, NY) at a delivered power of 50 W and in 80 % pulsed mode for 15 min.[28, 30, 31] Samples from the suspensions were then transferred into disposable 3 mL polystyrene cuvettes and shipped to NIST for measurement of the total Ti concentration. A minimum of three individual samples were tested from each suspension. spICP-MS analysis was also conducted on separately prepared samples. For the TEM specimen preparation, ≈5 µL of the TiO_2 suspension was pipetted onto TEM grids (200 mesh, Ted Pella, Redding, CA) and allowed to dry. The samples were then characterized using a JEOL 2000FX TEM operating at an accelerating voltage of 200 kV. Characterizations results including TEM, DLS, and ICP-OES analyses of the suspended NPs and

BPs is provided in the Supporting Information (SI) and in Figure S1 and Tables S1 and S2. While the DLS size measurements showed an average agglomerate size of greater than 100 nm for the TiO_2 NPs, TEM and spICP-MS analyses indicated that the majority of the particles were typically less than 100 nm.

Plant cultivation and exposure assay

Rice seeds (*Oryza sativa* L., Nipponbare) were obtained from the USDA Dale Bumpers National Rice Research Center (Stuttgart, Arkansas). Following surface sterilization in a 5 % bleach solution for 15 min and heat stimulation in a 50 ºC water bath for 4 h, seeds were allowed to germinate on moist filter papers in sterile Petri dishes until the development of the first true leaf. Selected uniform rice seedlings were then transplanted into aerated hydroponic pots in a greenhouse (University of Massachusetts, Amherst). Rice plants grew under the controlled average temperature of 24 ºC and 18 ºC during the day and night, respectively, with 4 h supplemental light after sunset (PAR source, 5.8 moles$\cdot m^{-2}\cdot d^{-1}$). Each pot was used to expose three rice plants after filling with 3.6 L Hoagland nutrient solution. The Hoagland media contained macronutrients (288 mg/L $NaNO_3$, 38 mg/L NaH_2PO_4, 446 mg/L KCl, 555 mg/L $CaCl_2$ and 240 mg/L $MgSO_4$) and micronutrients (0.5 mg/L H_3BO_3, 0.5 mg/L $MnCl_2\cdot 4H_2O$, 0.05 mg/L $ZnSO_4\cdot 7H_2O$, 0.02 mg/L $CuSO_4\cdot 5H_2O$, 0.01 mg/L $H_2MoO_4\cdot H_2O$ and 1.0 mg/L NaFe-EDDHA).

After assimilation for 3 d in Hoagland solution, the rice plants were exposed to nominal concentrations of 0, 5 mg/L and 50 mg/L TiO_2 NPs (prepared in Milli-Q water) for 24 h in separate glass containers wrapped with aluminum foil, while 5 mg/L and 50 mg/L TiO_2 BPs were used for comparison. Each treatment had 7 identical containers as replicates, and each container had 5 plants. After exposure for 24 h, some plants from each container were used for DNA damage[29, 32, 33] and antioxidant enzyme activity analyses. A description of the methods and results are described in the SI. The remaining plants were carefully rinsed and transferred to Hoagland nutrient solution without TiO_2 and were then incubated for another 3 days after which point they

were used for EM, total Ti, spICP-MS, and antioxidant enzyme activity analyses. Upon harvest, the plants were rinsed with running distilled water for at least 5 min, dried with paper towels using intermittent blotting, and then rinsed with running deionized water. For total Ti analysis, rice plants were separated into roots and leaves, digested with nitric and hydrofluoric acid, and analyzed using ICP-OES as described in the SI. For spICP-MS analysis, the roots and shoots were combined from several plants. The plant samples were treated with enzymatic (Macerozyme R-10) or acidic (12 mL of a 3:1 by volume mixture of concentrated nitric and hydrochloric acid) microwave digestion approaches prior to spICP-MS analysis; full details for the digestion approaches and spICP-MS analysis are provided in the SI. The actual concentration that the plants were exposed to and the settling of the NPs or BPs in the absence or presence of a plant for 24 h was analyzed using ICP-OES as described in the SI. Samples were taken immediately after sonication for the initial samples, while 20 mL samples were taken later after 24 h of settling in containers with or without plants to assess changes in the TiO_2 particle concentration during the exposure interval.

Analysis of TiO_2 nanoparticle uptake using scanning transmission electron microscopy

Roots and shoots were sampled for direct observation of TiO_2 NPs *in vivo*. Tissues were pre-fixed in monobasic phosphate buffer containing 4 % formaldehyde and 1 % glutaraldehyde (pH 7.2 to pH 7.4) for 2 h under vacuum, and post-fixed in 1 % osmium tetroxide/0.1 mol/L phosphate buffer for 1 h at room temperature. Subsequently, tissues were rinsed with a graded ethanol series (50 % to 100 % ethanol) and then with acetone. Following infiltration and embedding with Spurr's low viscosity resin,[33, 34] the epoxy resin was polymerized in a 60 °C oven for 24 h. Blocks containing plant tissues were sectioned on an ultracut microtome (Ultracut E, Reicher-Jung) to provide 60 nm to 90 nm thin sections and loaded onto 200 mesh uncoated copper grids. Sample stubs were placed in an environmental scanning electron microscope

(Quanta 200F, FEI, Hillsboro, OR), operating at high vacuum, for both imaging and compositional analysis via X-ray EDS (EDAX, Inc.).

Statistical Analysis

All analyses were conducted using GraphPad Prism (version 5). ICP-OES, DNA damage, and oxidative biomarker data were tested for outliers using the Grubb's test. For conditions with n=3, the data also had to deviate more than 50 % from the next closest value before being removed as an outlier. Significant differences among conditions were statistically analyzed using one-way ANOVA followed by Tukey's multiple comparison test for comparison among all sample sets or Dunnett's multiple comparison test for comparisons only against the control treatment; all samples analyzed statistically had at least three data points. Statistical significance (when not specified) was based on a probability of $p<0.05$.

Results and Discussion

STEM imaging of TiO_2 NPs

The roots and leaves from plants treated with 50 mg/L TiO_2 NPs were sampled and analyzed with STEM-EDS. There were no noticeable morphology changes in rice plants. STEM analysis showed that TiO_2 NPs extensively covered the root epidermal surface (Figure 1B,C,D). The accumulation on the epidermal surface may be through mechanical adhesion or diffusion, a finding previously observed with ZnO NPs and CeO_2 NPs or CuO NPs on the roots of corn or wheat plants, respectively.[35-39] Within the cytoplasm of the treated roots, electron dense dark deposits were recognized occasionally and confirmed to be elemental Ti through EDS analysis (Figure 1). These Ti-rich deposits were not observed in control plants (not shown). While the distribution of intracellular TiO_2 NPs followed no clear pattern, particles were more frequently found in root outer layers and tended to appear as agglomerates near plasma membranes (Figure 1D,E). In wheat (*Triticum aestivum spp.*), it was also observed that TiO_2 NPs (exposure at 100 mg/L) were

entrapped in endosome or vacuole-like structures.[15] Unlike what was reported for wheat, TiO_2 NP clusters in rice roots did not show affinity for certain cell organelles, but appeared as free NPs close to plasma membranes. In a study on the uptake of TiO_2 using cucumber (*Cucumis sativus*), TiO_2 particles were found using micro X-ray fluorescence and micro X-ray absorption spectroscopy to penetrate into the transport system.[18, 40] In agreement with those results obtained from exposed cucumber and wheat, TiO_2 NPs were able to penetrate rice roots and enter into root cells as confirmed through STEM-EDS, which is the first direct evidence of TiO_2 NPs uptake in rice plant root cells. This solid evidence of TiO_2 internalization by plant cells was also consistent with a variety of other metal-based nanoparticles, including Fe_3O_4, Au and Cu nanoparticles.[41-45] Intracellular TiO_2 NP clusters may result from the agglomeration of internalized individual particulates under the dynamic physiological environment in the cytoplasm.

After internalization, TiO_2 NPs have the potential to translocate into the shoots and even into edible regions. However, no obvious accumulation of TiO_2 clusters was observed in rice leaf tissues through STEM observation, probably due to limited transfer from roots to shoot and the lower exposure concentration relative to other studies.[15, 18] Larue *et al.* reported 36 nm as the upper threshold diameter for TiO_2 NPs to translocate from root to leaves in wheat, while Servin *et al.* used micro-x-ray absorption near edge spectroscopy spectra to reveal the presence of TiO_2 NPs (Degussa P25) in cucumber leaf tissues suggesting that larger agglomerates similar to those prepared in this study can also be internalized by some plants.[15, 18] TiO_2 NPs have negligible ion release at the pH used in this study and are reported to remain in the same chemical form *in vivo*,[18, 46, 47] a result confirmed in this study through elemental analysis after filtering particle suspensions that had been acid treated and not finding detectable dissolved Ti (see SI). Thus, it is improbable that Ti ions were absorbed into the plants and then reformed into particles.

Trends in titanium accumulation in plant tissues

With the evidence of observable TiO_2 NPs in rice plants, ICP-OES was further employed to quantify the element accumulation over time in the roots and shoots (Figure 2). Titanium

accumulated in the shoots at a considerably lower level than in the roots, with a roughly two orders of magnitude difference. Despite vigorously washing the roots, this difference may partly stem from the titanium root concentration including particles adhering to the external surfaces of the roots in addition to particles inside the roots, while the concentration measured in the stems only included internalized titanium.

Characterization of TiO_2 NP and BP uptake using spICP-MS

In addition to characterizing the total Ti in the plant tissues, it is important to assess the size distribution and number concentration of the particles in the tissues. This was accomplished via spICP-MS analysis using two different extraction methods: microwave acid digestion and an enzymatic digestion that was previously used to extract gold NPs from tomato plants.[19]

According to multiple control measurements, neither the enzymatic nor acid digestion procedures clearly changed the size distribution of the NPs or BPs (Figure 3 and S2 and Tables 1 and 2). For the NP treatment, an increase in the value for the smallest bin size above the background was observed for the acid-treated control samples (Figure 3B compared to 3A; 32 nm increased to 47 nm) but not the enzyme-treated samples (Figure 3E compared to 3D). The size detection limit was determined by background counts in the control medias, but some of the detection limit variation may be due to slight daily changes in instrument performance. Importantly, the size detection limit was not impacted by dissolved Ti; measurements of the dissolved Ti concentration determined by ICP-OES analysis of the NPs following the acid digestion treatment and filtration with a 0.02 µm pore size filter were never greater than the instrument detection limit (0.0006 mg/L Ti). Reagent control samples (without particles) did show a small number of pulses that were above the background cutoff and were interpreted as particles, but most of these pulses were just above the background cut-off and therefore were interpreted as NPs just above the size detection limit (Figure S3, S4, and S5). The presence of a small number of large pulses in the control matrix is not surprising given that analysis of water or 2% nitric acid blank yields a small number of peaks (5 to 50) during a 60 second analysis when

analyzing for Ti. The peaks observed in blanks are thought to be dust or particles that were located in the sample introduction system and became dislodged during sample analysis (Figure S4 and S5). In this experiment, the acid matrix showed an average of 42 ± 11 peaks during a 60 s run and the 24 h enzyme matrix was slightly higher with an average of 77 ± 20 peaks; Figure S4 shows a comparison between the acid matrix and the number of spikes for a NP exposed plant treated with the acid digestion approach. It is also important to note the total Ti in controls (spICP-MS data shown in Figures S3 and S4) is below or at the limit of detection when doing total elemental analysis of Ti. Treatment of control plant samples (not exposed to particles) resulted in spikes that could be interpreted as particles, with an average of 390 ± 190 peaks in the enzyme digestion samples and 150 ± 112 peaks in the acid digestion samples. In comparison, the number of peaks detected in NP exposed plant samples was 5080 ± 1970 and 2390 ± 1850 pulses for the acid digestion and 24 h enzyme digestion, respectively. Figure 4 shows the size distribution of these apparent particles in the control plants. Although there were more peaks in the enzyme digested control plants, the particles are calculated to be near the size detection limit, probably outliers in background signal that were not removed during data processing (Figure 4). The pulses in the acid treatment of the control plants were larger. The instrumental transport efficiency and dilution factors were used to calculate how many particles were detected per plant for control, NP-exposed, and BP-exposed plants by each digestion method (Table S3). In the acid treatment, there are approximately 50 x more particles in the NP-exposed plants and 5 x more particles in the BP-exposed plants than in the control plants.

For the NP-exposed plants treated with the acid digestion process, there was an increase in the breadth of the distribution (Figure 3C and S6C) as indicated by a greater number of particles in the tail to the right of the main distribution. This result contrasts with the data from the enzymatic digested NP-exposed plants, which show distributions more similar to those of the NP control (without NP or BP exposure) (Figures 3 and S3). While there is an increase in frequency for the 24 h and 48 h enzymatic treatments in the range of 45 nm to 60 nm for these samples as

compared to the NP control treatments, this result could be impacted by the background subtraction process. The broader size distribution of the NP-exposed plants after treatment with the acid digestion process could stem from changes to the NPs caused by the acid treatment or as a result of the enzymatic process being a less efficient extraction process of the plant tissues and not liberating larger particles that were associated with the plant tissue; however, control experiments did not show a change in the size distribution to the NPs after the acid treatment (Figure 3). It was clear from visual inspection that a larger fraction of undigested plant material remained after the enzymatic process and the average total amount of Ti extracted from the plants was approximately 6 x higher for the acid digestion compared to the enzymatic digestion as determined by integrating and summing the spICP-MS peaks.

The plants exposed to the BP treatment showed a similar size distribution for the acid digestion procedure to BP controls in ultra-pure water, while a substantially higher frequency of smaller particles was observed for the 24 h and 48 h enzyme extraction procedure (Figures 3, S3, and S6), a result similar to that observed for the NP-exposed plants. The increase in the number of smaller particles for the enzymatic extraction procedures may be partially due to the background cut-off procedure not removing some background counts or from the enzyme process being less efficient than the acid digestion procedure with regards to extracting larger particles. The macerozyme is a mixture of cellulase, hemicellulase, and pectinase, and is designed to break down the cell walls of plant cells. Since there was still plant matter clearly visible in the digestion following 48 h, it is possible that not all cell walls were destroyed and perhaps remained sufficiently intact to retain the larger BPs.

Overall, both acid and enzyme digestion methods successfully extracted particles from the plant tissues, and there was a clear difference in size distribution of extracted TiO_2 particles for the plants exposed to the BPs and NPs. The size distribution for the NP exposed plants had a narrower size distribution which contained predominately smaller particles while the BP exposed

plants showed a much broader distribution with a larger fraction of particles with sizes greater than 100 nm. This indicates that spICP-MS was able to identify a difference in the particle size distribution among the NP and BP treatments, which is a finding that could not be readily obtained using total elemental analysis or electron microscopy. However, the precision of this result was impacted by limitations regarding the efficiency of the enzymatic digestion procedures for particles with larger sizes and uncertainty from the background subtraction step for particles smaller than $\approx$55 nm. The value of EM analysis is that it provided definitive identification of the NPs in the plant tissues and also information about the distribution of the NPs within the tissues, but only a small fraction of the plant area can be analyzed within a reasonable time period. Total elemental analysis also provided complementary information to spICP-MS given that the recovery of the Ti from the digestion procedure could be readily quantified such as by comparing the concentration measured using ICP-OES to the concentration from an orthogonal Ti quantification methods (e.g., neutron activation analysis). However, orthogonal methods are not yet available for comparison of the size distribution of NPs measured after spICP-MS extractions, but the total quantity of Ti measured after different extraction procedures and spICP-MS analysis could be compared to that for the total elemental analysis. Overall, each technique provided important, complementary insights into the bioaccumulation behaviors of NPs and BPs within the rice plant.

ASSOCIATED CONTENT

Supporting Information. Supplemental methods, supplemental results and discussion, and nine figures and three tables are included in the Supporting Information. This material is available free of charge via the Internet at http://pubs.acs.org.

ACKNOWLEDGEMENTS

This research was supported by USDA NIFA Hatch Program (MAS 00475) and EPA grant RD83558001. Mention of trade names or commercial products is solely for the purpose of providing specific information and does not imply recommendation or endorsement by the National Institute of Standards and Technology. We thank Vincent Hackley and Julian Taurozzi (NIST) for providing samples of SRM 1898 and for assistance with the dispersion protocol.

333 Table 1: spICP-MS analysis of the enzyme digestion samples (n=3).

Sample	Mean Diameter ± Standard Deviation (nm)	Mode Diameter (nm)
NP in MilliQ (no treatment)	79 ± 30	48
BP in MilliQ (no treatment)	161 ± 60	206
24h Enzyme Digestion Treated Samples		
Enzyme Only Control (no added particles)	81 ± 49	43
Control Plants	58 ± 30	42
NP in Enzyme	78 ± 28	56
Plants Exposed to NPs	71 ± 31	44
BP in Enzyme	145 ± 62	74
Plants Exposed to BPs	107 ± 66	42
48h Enzyme Digestion Treated Samples		
Enzyme Only Control (no added particles)	70 ± 30	50
Control Plant	68 ± 35	48
NP in Enzyme	76 ± 29	48
Plants Exposed to NPs	70 ± 30	42
BP in Enzyme	136 ± 56	84
Plants Exposed to BPs	116 ± 63	60

334

335 Table 2: spICP-MS analysis of the acid-digestion samples (n=3).

Sample	Mean Diameter ± Standard Deviation (nm)	Mode Diameter (nm)
NP in MilliQ(no treatment)	78 ± 38	34
BP In MilliQ(no treatment)	150 ± 65	95
Acid Digestion Treated Samples		
Acid Control (no added particles)	112 ± 65	58
Control Plants	124 ± 57	60
NP in Acid	94 ± 36	52
Plants Exposed to NPs	126 ± 53	65
BP in Acid	159 ± 67	128
Plants Exposed to BPs	181 ± 67	236

336

337
338

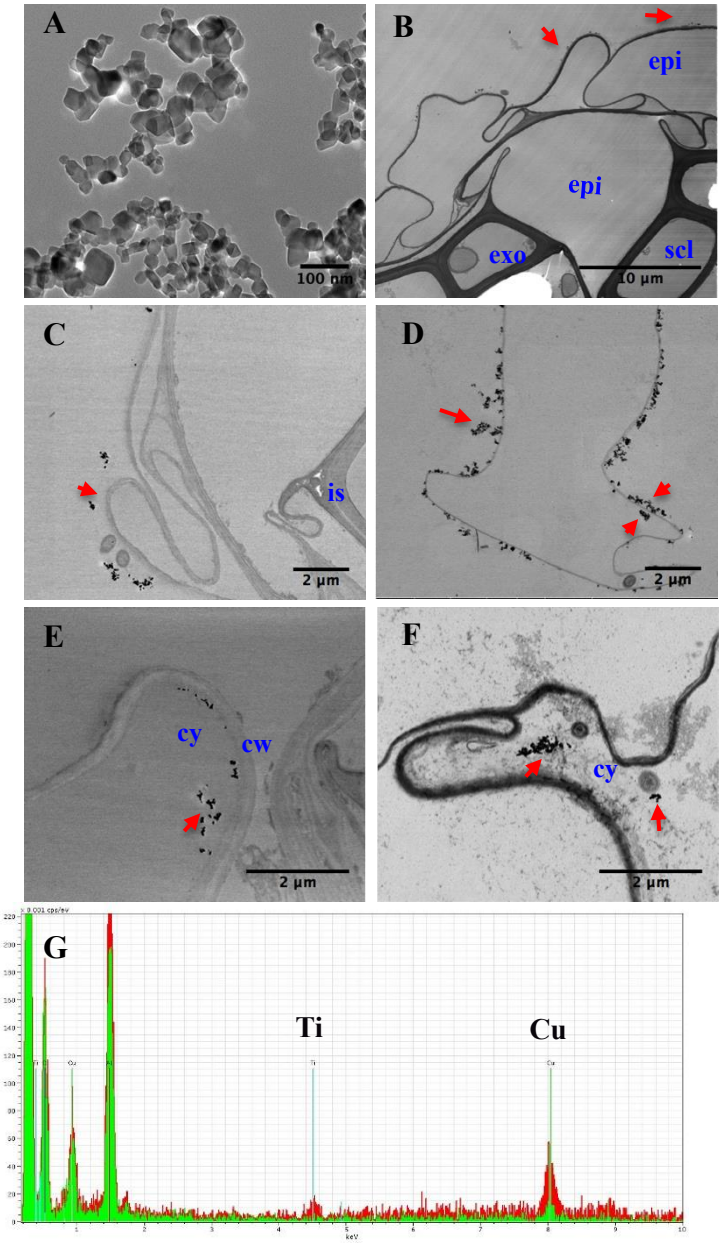

339

340

341 Figure 1. Transmission electron micrographs of TiO_2 NPs under 20 kV. (A) TiO_2 NPs were characterized in
342 Milli-Q water; (B-F) Transverse root sections of rice (*Oryza sativa* L.) grown in 50 mg/L TiO_2 NP
343 suspension for 24 h were observed under STEM-EDS. Microstructure, as denoted in blue, included
344 exodermis (exo), sclerenchyma (scl), epidermis (epi), cell wall (cw), intercellular space (is) and cytoplasm
345 (cy). Condensed dark spots, shown with red arrow, represented TiO_2 NPs and were identified as Ti through
346 energy-dispersive spectroscopy. In the EDS figure (G), the red spectrum is an example of an area with
347 Ti-containing particles while the green spectrum is a background spectrum that does not contain
348 nanoparticles. Copper signals come from the grids.

349

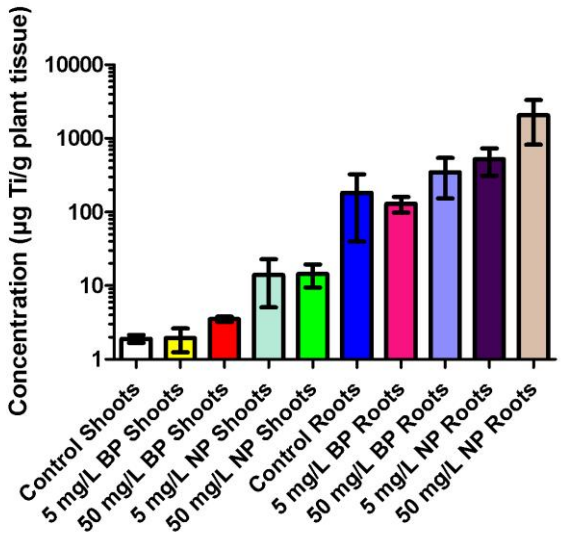

Figure 2. Titanium accumulation in rice roots (A) and shoots (B) resulting from TiO_2 NP and BP exposure. Each data point represents the mean ± SD, for 2 or 3 samples (plantlets were combined into 3 replicates but some results were removed as a result of being outliers). Note the logarithmic scale for the y-axis.

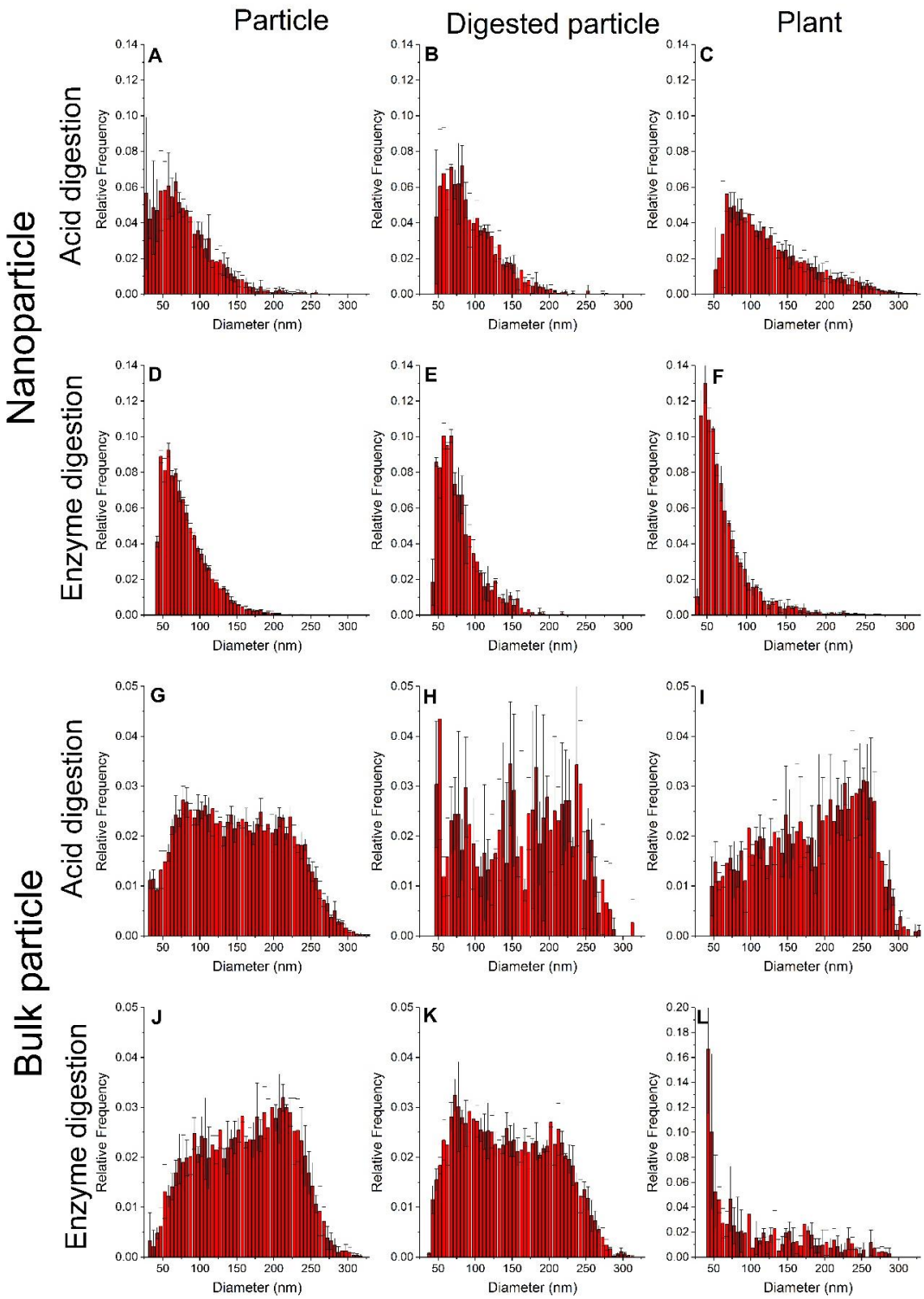

355

356 Figure 3: spICP-MS analysis of the acid digestion and 24 h enzyme digestion treatments for the
357 samples. Size distributions are normalized to relative frequency. All graphs are the averages of
358 triplicate samples and error bars represent standard deviation values. Particles dispersed in water

without treatment for NPs (A & D) and BPs (G & J). The results shown in part A and G versus D and J were from samples analyzed on the same day as the samples which were treated with the acid digestion and enzyme extraction, respectively. Differences between the results reflect the day-to-day variability in spICP-MS analysis of TiO_2 NPs. NPs which were acid digested (B) or digested using enzymes for 24 h (E). BPs which were acid digested (H) or digested using enzymes for 24 h (K). Microwave acid digested plants which were exposed to NPs (C) or BPs (I). Plants exposed to NPs (F) or BPs (L) following 24h of enzyme digestion. The samples in parts A, B, C, G, H, and I were analyzed the same day as were the samples in parts D, E, F, J, K and L. Changes in the size detection limit were not from dissolved Ti in either digestion.

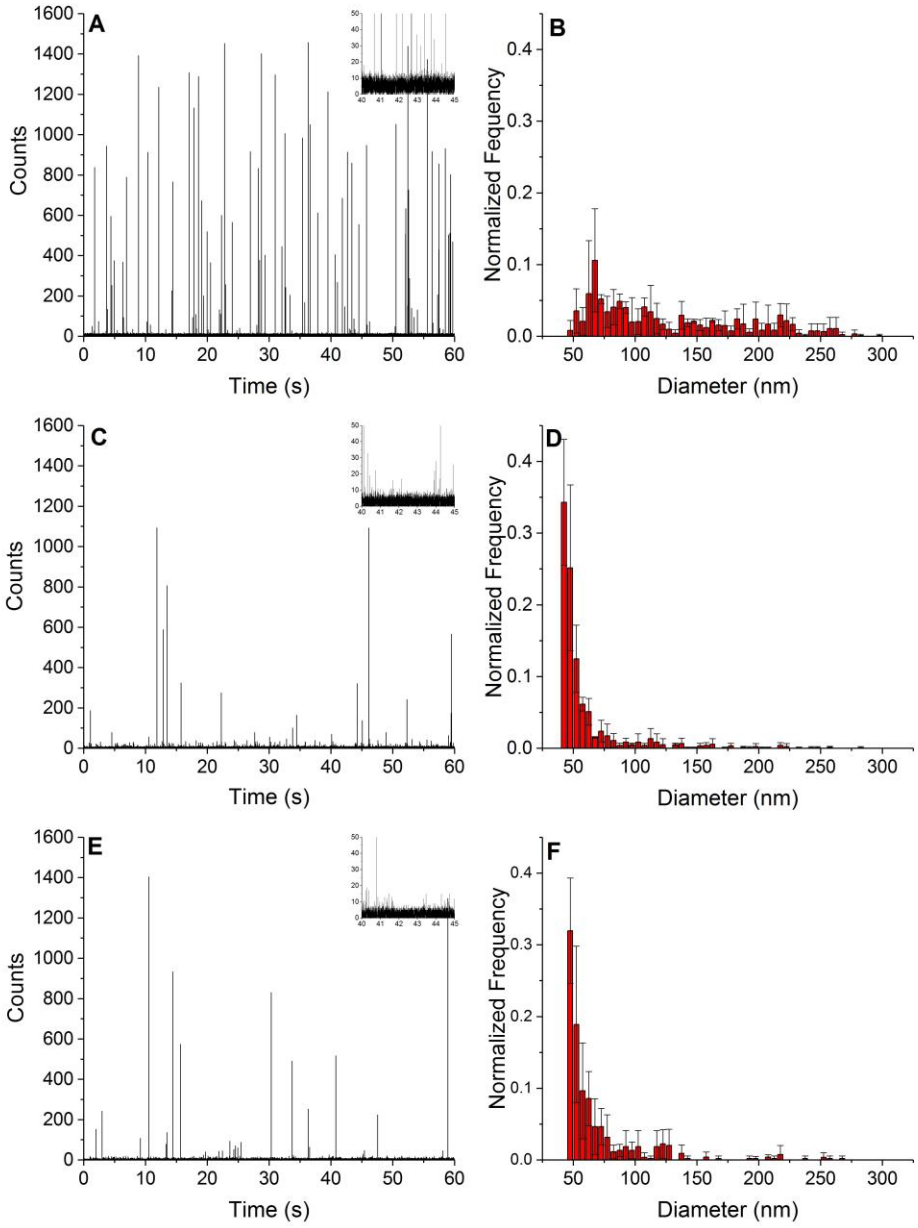

369

370 Figure 4: Example graphs of raw single particle data, pulses are interpreted as particles, for
371 digestion of control plants using acid (A), 24 h enzymatic (C), or 48 h enzymatic (E) treatments.
372 Insets zoom in on five seconds of data to reveal the background. Relative frequency for
373 digestion of control plants using acid (B), 24 h enzymatic (D), or 48 h enzymatic (F) treatments;
374 graphs are the averages of triplicate samples and error bars represent standard deviation values.

References

1. Weir, A.; Westerhoff, P.; Fabricius, L.; Hristovski, K.; von Goetz, N., Titanium Dioxide Nanoparticles in Food and Personal Care Products. *Environ Sci & Tech* **2012,** *46*, (4), 2242-2250.
2. Chen, X.; Mao, S. S., Titanium Dioxide Nanomaterials: Synthesis, Properties, Modifications, and Applications. *Chem. Rev.* **2007,** *107*, (7), 2891-2959.
3. Gottschalk, F.; Sonderer, T.; Scholz, R. W.; Nowack, B., Modeled Environmental Concentrations of Engineered Nanomaterials (TiO2, ZnO, Ag, CNT, Fullerenes) for Different Regions. *Environ Sci & Tech* **2009,** *43*, (24), 9216-9222.
4. Gottschalk, F.; Sun, T. Y.; Nowack, B., Environmental concentrations of engineered nanomaterials: Review of modeling and analytical studies. *Environ. Pollut.* **2013,** *181*, 287-300.
5. Mueller, N. C.; Nowack, B., Exposure modeling of engineered nanoparticles in the environment. *Environ Sci & Tech* **2008,** *42*, (12), 4447-4453.
6. Musee, N., Simulated environmental risk estimation of engineered nanomaterials: A case of cosmetics in Johannesburg City. *Hum Exp Toxicol* **2011,** *30*, (9), 1181-1195.
7. Cai, F.; Wu, X.; Zhang, H.; Shen, X.; Zhang, M.; Chen, W.; Gao, Q.; White, J. C.; Tao, S.; Wang, X., Impact of TiO 2 nanoparticles on lead uptake and bioaccumulation in rice (Oryza sativa L.). *NanoImpact* **2017,** *5*, 101-108.
8. Tripathi, D. K.; Singh, S.; Singh, V. P.; Prasad, S. M.; Chauhan, D. K.; Dubey, N. K., Silicon Nanoparticles More Efficiently Alleviate Arsenate Toxicity than Silicon in Maize Cultiver and Hybrid Differing in Arsenate Tolerance. *Front Environ Sci* **2016,** *4*, 46.
9. Liu, H.; Ma, C.; Chen, G.; White, J. C.; Wang, Z.; Xing, B.; Dhankher, O. P., Titanium Dioxide Nanoparticles Alleviate Tetracycline Toxicity to Arabidopsis thaliana (L.). *ACS Sustainable Chemistry & Engineering* **2017,** *5*, (4), 3204-3213.
10. Bandyopadhyay, S.; Peralta-Videa, J. R.; Gardea-Torresdey, J. L., Advanced Analytical Techniques for the Measurement of Nanomaterials in Food and Agricultural Samples: A Review. *Environ Eng Sci* **2013,** *30*, (3), 118-125.
11. Zhang, Z.; Guo, H.; Deng, Y.; Xing, B.; He, L., Mapping gold nanoparticles on and in edible leaves in situ using surface enhanced Raman spectroscopy. *RSC Adv.* **2016,** *6*, (65), 60152-60159.
12. Hassellov, M.; Readman, J. W.; Ranville, J. F.; Tiede, K., Nanoparticle analysis and characterization methodologies in environmental risk assessment of engineered nanoparticles. *Ecotoxicology* **2008,** *17*, (5), 344-361.
13. Handy, R. D.; van den Brink, N.; Chappell, M.; Muehling, M.; Behra, R.; Dusinska, M.; Simpson, P.; Ahtiainen, J.; Jha, A. N.; Seiter, J.; Bednar, A.; Kennedy, A.; Fernandes, T. F.; Riediker, M., Practical considerations for conducting ecotoxicity test methods with manufactured nanomaterials: what have we learnt so far? *Ecotoxicology* **2012,** *21*, (4), 933-972.
14. Kurepa, J.; Paunesku, T.; Vogt, S.; Arora, H.; Rabatic, B. M.; Lu, J. J.; Wanzer, M. B.; Woloschak, G. E.; Smalle, J. A., Uptake and Distribution of Ultrasmall Anatase TiO2 Alizarin Red S Nanoconjugates in Arabidopsis thaliana. *Nano Lett.* **2010,** *10*, (7), 2296-2302.
15. Larue, C.; Laurette, J.; Herlin-Boime, N.; Khodja, H.; Fayard, B.; Flank, A. M.; Brisset, F.; Carriere, M., Accumulation, translocation and impact of TiO2 nanoparticles in wheat (Triticum aestivum spp.): Influence of diameter and crystal phase. *Sci Total Environ* **2012,** *431*, 197-208.
16. Larue, C.; Pinault, M.; Czarny, B.; Georgin, D.; Jaillard, D.; Bendiab, N.; Mayne-L'Hermite, M.; Taran, F.; Dive, V.; Carriere, M., Quantitative evaluation of multi-walled carbon nanotube uptake in wheat and rapeseed. *J Hazard Mater* **2012,** *227*, 155-163.

17. Fan, R. M.; Huang, Y. C.; Grusak, M. A.; Huang, C. P.; Sherrier, D. J., Effects of nano-TiO2 on the agronomically-relevant Rhizobium-legume symbiosis. *Sci Total Environ* **2014,** *466*, 503-512.
18. Servin, A. D.; Castillo-Michel, H.; Hernandez-Viezcas, J. A.; Diaz, B. C.; Peralta-Videa, J. R.; Gardea-Torresdey, J. L., Synchrotron Micro-XRF and Micro-XANES Confirmation of the Uptake and Translocation of TiO2 Nanoparticles in Cucumber (Cucumis sativus) Plants. *Environ Sci & Tech* **2012,** *46*, (14), 7637-7643.
19. Dan, Y.; Zhang, W.; Xue, R.; Ma, X.; Stephan, C.; Shi, H., Characterization of Gold Nanoparticle Uptake by Tomato Plants Using Enzymatic Extraction Followed by Single-Particle Inductively Coupled Plasma–Mass Spectrometry Analysis. *Environ Sci & Tech* **2015,** *49*, (5), 3007-3014.
20. Dan, Y.; Ma, X.; Zhang, W.; Liu, K.; Stephan, C.; Shi, H., Single particle ICP-MS method development for the determination of plant uptake and accumulation of CeO2 nanoparticles. *Anal Bioanal Chem* **2016,** *408*, (19), 5157-5167.
21. Donovan, A. R.; Adams, C. D.; Ma, Y.; Stephan, C.; Eichholz, T.; Shi, H., Single particle ICP-MS characterization of titanium dioxide, silver, and gold nanoparticles during drinking water treatment. *Chemosphere* **2016,** *144*, 148-153.
22. Vidmar, J.; Milačič, R.; Ščančar, J., Sizing and simultaneous quantification of nanoscale titanium dioxide and a dissolved titanium form by single particle inductively coupled plasma mass spectrometry. *Microchem. J.* **2017,** *132*, 391-400.
23. Dan, Y.; Shi, H.; Stephan, C.; Liang, X., Rapid analysis of titanium dioxide nanoparticles in sunscreens using single particle inductively coupled plasma–mass spectrometry. *Microchem. J.* **2015,** *122*, 119-126.
24. Pace, H. E.; Rogers, N. J.; Jarolimek, C.; Coleman, V. A.; Higgins, C. P.; Ranville, J. F., Determining Transport Efficiency for the Purpose of Counting and Sizing Nanoparticles via Single Particle Inductively Coupled Plasma Mass Spectrometry. *Anal. Chem.* **2011,** *83*, (24), 9361-9369.
25. Montano, M. D.; Badiei, H. R.; Bazargan, S.; Ranville, J. F., Improvements in the detection and characterization of engineered nanoparticles using spICP-MS with microsecond dwell times. *Environ Sci Nano* **2014,** *1*, (4), 338-346.
26. Montoro Bustos, A. R.; Petersen, E. J.; Possolo, A.; Winchester, M. R., Post hoc Interlaboratory Comparison of Single Particle ICP-MS Size Measurements of NIST Gold Nanoparticle Reference Materials. *Anal. Chem.* **2015,** *87*, (17), 8809-8817.
27. El Hadri, H.; Petersen, E. J.; Winchester, M. R., Impact of and correction for instrument sensitivity drift on nanoparticle size measurements by single-particle ICP-MS. *Anal Bioanal Chem* **2016,** *408*, (19), 5099-5108.
28. Taurozzi, J. S.; Hackley, V. A.; Wiesner, M. R., A standardised approach for the dispersion of titanium dioxide nanoparticles in biological media. *Nanotoxicology* **2013**, 7, (4), 389-401.
29. Petersen, E. J.; Reipa, V.; Watson, S. S.; Stanley, D. L.; Rabb, S. A.; Nelson, B. C., DNA Damaging Potential of Photoactivated P25 Titanium Dioxide Nanoparticles. *Chem Res Toxicol* **2014,** *27*, (10), 1877-1884.
30. Taurozzi, J. S.; Hackley, V. A.; Wiesner, M. R., Ultrasonic dispersion of nanoparticles for environmental, health and safety assessment - issues and recommendations. *Nanotoxicology* **2011,** *5*, (4), 711-729.
31. J. S. Taurozzi, V. A. H., M. R. Wiesner Preparation of Nanoscale TiO2 Dispersions in Biological Test Media for Toxicological Assessment. http://dx.doi.org/10.6028/NIST.SP.1200-4
32. Petersen, E. J.; Nelson, B. C., Mechanisms and measurements of nanomaterial-induced oxidative damage to DNA. *Anal Bioanal Chem* **2010,** *398*, (2), 613-650.

33. Atha, D. H.; Wang, H. H.; Petersen, E. J.; Cleveland, D.; Holbrook, R. D.; Jaruga, P.; Dizdaroglu, M.; Xing, B. S.; Nelson, B. C., Copper Oxide Nanoparticle Mediated DNA Damage in Terrestrial Plant Models. *Environ Sci & Tech* **2012,** *46*, (3), 1819-1827.
34. Spurr, A. R., A low-viscosity epoxy resin embedding medium for electron microscopy. *J Ultrastruct Res* **1969,** *26*, (1–2), 31-43.
35. Lin, D.; Xing, B., Root uptake and phytotoxicity of ZnO nanoparticles. *Environ Sci & Tech* **2008,** *42*, (15), 5580-5585.
36. Wild, E.; Jones, K. C., Novel Method for the Direct Visualization of in Vivo Nanomaterials and Chemical Interactions in Plants. *Environ Sci & Tech* **2009,** *43*, (14), 5290-5294.
37. Zhao, L. J.; Peralta-Videa, J. R.; Ren, M. H.; Varela-Ramirez, A.; Li, C. Q.; Hernandez-Viezcas, J. A.; Aguilera, R. J.; Gardea-Torresdey, J. L., Transport of Zn in a sandy loam soil treated with ZnO NPs and uptake by corn plants: Electron microprobe and confocal microscopy studies. *Chem Eng J* **2012,** *184*, 1-8.
38. Deng, Y. Q.; White, J. C.; Xing, B. S., Interactions between engineered nanomaterials and agricultural crops: implications for food safety. *J Zhejiang Univ Sci* **2014,** *15*, (8), 552-572.
39. Zhou, D.; Jin, S.; Li, L.; Wang, Y.; Weng, N., Quantifying the adsorption and uptake of CuO nanoparticles by wheat root based on chemical extractions. *J Environ Sci China* **2011,** *23*, (11), 1852-1857.
40. Servin, A. D.; Morales, M. I.; Castillo-Michel, H.; Hernandez-Viezcas, J. A.; Munoz, B.; Zhao, L.; Nunez, J. E.; Peralta-Videa, J. R.; Gardea-Torresdey, J. L., Synchrotron Verification of TiO2 Accumulation in Cucumber Fruit: A Possible Pathway of TiO2 Nanoparticle Transfer from Soil into the Food Chain. *Environ Sci & Tech* **2013,** *47*, (20), 11592-11598.
41. Gardea-Torresdey, J. L.; Rico, C. M.; White, J. C., Trophic Transfer, Transformation, and Impact of Engineered Nanomaterials in Terrestrial Environments. *Environ Sci & Tech* **2014,** *48*, (5), 2526-2540.
42. Zhu, H.; Han, J.; Xiao, J. Q.; Jin, Y., Uptake, translocation, and accumulation of manufactured iron oxide nanoparticles by pumpkin plants. *J Environ Monit* **2008,** *10*, (6), 713-717.
43. Judy, J. D.; Unrine, J. M.; Rao, W.; Wirick, S.; Bertsch, P. M., Bioavailability of Gold Nanomaterials to Plants: Importance of Particle Size and Surface Coating. *Environ Sci & Tech* **2012,** *46*, (15), 8467-8474.
44. Sabo-Attwood, T.; Unrine, J. M.; Stone, J. W.; Murphy, C. J.; Ghoshroy, S.; Blom, D.; Bertsch, P. M.; Newman, L. A., Uptake, distribution and toxicity of gold nanoparticles in tobacco (Nicotiana xanthi) seedlings. *Nanotoxicology* **2012,** *6*, (4), 353-360.
45. Lee, W. M.; An, Y. J.; Yoon, H.; Kweon, H. S., Toxicity and bioavailability of copper nanoparticles to the terrestrial plants mung bean (Phaseolus radiatus) and wheat (Triticum aestivum): Plant agar test for water-insoluble nanoparticles. *Environ Toxicol Chem* **2008,** *27*, (9), 1915-1921.
46. David Holbrook, R.; Motabar, D.; Quiñones, O.; Stanford, B.; Vanderford, B.; Moss, D., Titanium distribution in swimming pool water is dominated by dissolved species. *Environ. Pollut.* **2013,** *181*, 68-74.
47. Wang, H.; Wick, R. L.; Xing, B., Toxicity of nanoparticulate and bulk ZnO, Al2O3 and TiO2 to the nematode Caenorhabditis elegans. *Environ. Pollut.* **2009,** *157*, (4), 1171-1177.